DTU Library

Interlayer Excitons with Large Optical Amplitudes in Layered van der Waals Materials

Deilmann, Thorsten; Thygesen, Kristian Sommer

Link back to DTU Orbit

Interlayer excitons with large optical amplitudes

in layered van der Waals materials

Thorsten Deilmann[*,†] and Kristian Sommer Thygesen[†]

†*CAMD, Department of Physics, Technical University of Denmark, DK-2800 Kongens Lyngby, Denmark*

‡*Center for Nanostructured Graphene (CNG), Technical University of Denmark, DK-2800 Kongens Lyngby, Denmark*

E-mail: thorsten.deilmann@wwu.de

Abstract

Vertically stacked two-dimensional materials form an ideal platform for controlling and exploiting light-matter interactions at the nanoscale. As a unique feature, these materials host electronic excitations of both intra- and interlayer type with distinctly different properties. In this Letter, using first-principles many-body calculations, we provide a detailed picture of the most prominent excitons in bilayer MoS_2 – a prototypical van der Waals material. By applying an electric field perpendicular to the bilayer, we explore the evolution of the excitonic states as the band alignment is varied from perfect line-up to staggered (Type II) alignment. For moderate field strengths, the lowest exciton has intralayer character and is almost independent of the electric field. However, we find higher lying excitons that have interlayer character. They can be described as linear combinations of the intralayer B exciton and optically dark charge transfer excitons and, interestingly, these mixed interlayer excitons have strong optical amplitude and can be easily tuned by the electric field. The first-principles results

can be accurately reproduced by a simple excitonic model Hamiltonian that can be straightforwardly generalised to more complex van der Waals materials.

Keywords

2D materials, heterostructures, interlayer excitons, optical amplitude, optional spectra, many-body perturbation theory

Two-dimensional (2D) materials and van der Waals heterostructures (consisting of vertically stacked 2D materials) are attracting enormous attention due to their unique and tunable properties which make them interesting for both applied and fundamental science.[1] In particular, mono- and few layer transition metal dichalcogenides (TMDCs) exhibit highly interesting optical properties many of which derive from their strongly bound excitons.[2] Over the past few years, the exploration of 2D excitons in TMDCs has advanced our understanding of electron-electron interactions in reduced dimensions[3–7] and enabled detailed studies of e.g. exciton dissociation,[8] exciton polaritons,[9] biexciton formation,[10] nonlinear effects,[11] and very recently the exciton Hall effect.[12]

While the physics of excitons in monolayer TMDCs is well developed, less is known about excitons in multilayer van der Waals (vdW) structures. One important effect of going from mono- to multilayer structures is that the screened interaction changes in a
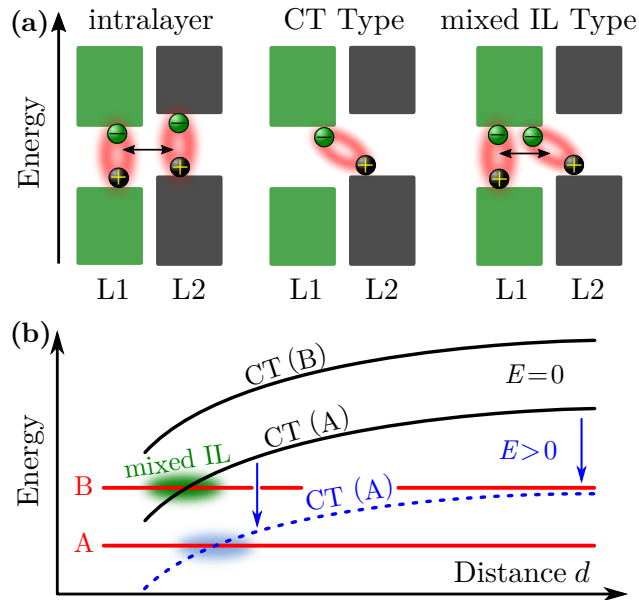
Figure 1: (a) Schematic representation of the composition of an intralayer excitation compared to the two different kinds of interlayer (IL) excitations on layer 1 (L1) and 2 (L2). The middle panel shows a CT Type exciton, and the right panel sketches a mixed IL Type exciton (mixing of intralayer and CT excitons). (b) Sketch of intralayer excitons A and B (red) and corresponding CT excitons (black for $E = 0$). If the states are close in energy mixed IL states can form (green). Applying an electrical field CT excitations can be shifted in energy (blue dashed line) and may form further mixed states.

non-trivial way.[13–15] But more interestingly, the multilayer structures can host new types of excitons where the electron and hole live on different layers. Quite generally, excitons in vdW multilayer structures can be categorised into two types according to whether the electron and hole always reside on the same layer (intralayer) or can be found on different layers (interlayer). Note that an intralayer exciton may extend over several layers (see Figure 1(a), left), but the motion of the electron and the hole is correlated such that they always reside on the same layer. A special type of interlayer exciton are the charge transfer (CT) excitons, where the electron and hole never reside on the same layer. These excitons are typical of vdW heterostructures with Type II band alignment (see Figure 1(a), middle) and have been discussed previously in coupled GaAs quantum wells.[16] In general, however, an interlayer exciton will have a lower degree of correlation between the electron and hole which consequently may be found on the same layer or on different layers (Figure 1(a), right). Such excitons may be described a linear combination of an intralayer and CT exciton, and are thus expected to form when two such excitons are almost degenerate. In Fig. 1(b) we show two intralayer excitons A and B and their corresponding CT excitations. As intralayer and CT states respond different on the interlayer distance and perpendicular electric fields their energetic alignment can be tuned.

Due to the strong spatial separation of the electron and hole in a CT exciton, such excitons have extraordinarily long lifetimes and are seen as potential candidates for realizing a wealth of interesting physical phenomena, such as Bose-Einstein condensation, high temperature superfluidity, dissipationless current flow, and the light-induced exciton spin Hall effect.[17–19] Such CT excitons have been observed in heterobilayers with a natural Type II band alignment[20–22] and in bilayer MoS_2 where the Type II band alignment is imposed by an electric field applied perpendicular to the bilayer.[23]

While the spatial separation of the electron and hole in the CT exciton leads to long lifetimes it also causes a small optical transition matrix element making it challenging to probe by them in absorption and luminescence experiments. On the other hand, interlayer

4

excitons with finite optical amplitudes have been recently identified in bulk MoS_2, $MoSe_2$, and $MoTe_2$[24,25] (by the different sign of the g-factors in magnetic fields compared to intralayer states).

While previous work has explored interlayer states of the CT Type in bilayer and few-layer systems,[26–30] mixed interlayer (IL) excitons of the type shown in Fig. 1(a, right), have not been discussed in detail. In this Letter we use first-principles many-body calculations to unravel the nature of all three possible types of the bound excitons in bilayer MoS_2. By applying an electric field perpendicular to the bilayer we explore the evolution of the different excitonic states as the band alignment between the monolayers is varied. We identify both intralayer as well as interlayer excitons with zero and finite optical amplitudes demonstrating the rich and tunable physics of excitons in even the simplest vdW structures. Finally, we consider a simple model Hamiltonian that captures the main features of interlayer exciton formation in vdW crystals.

We begin by considering the band structure of bilayer MoS_2 in an applied electric field [Fig. 2(a)] [1]. The computational details are discussed in the supplement. The bilayer at zero field (black line) shows an indirect gap between Γ and a minimum on the K-Γ line. However, the direct gap remains at K as in the monolayer.[32,33] For small field strengths (E_z) the main changes in the band structure occur around the K point (marked by blue circles) where the interlayer hybridisation is weak. As the lowest lying optically bright excitons are mainly formed by electron-hole pairs around K, the electric field is expected to influence these excitons. In Figs. 2(b) and (c) we show the dependence of the lowest conduction bands (CB) and highest valence bands (VB) at the K-point with respect to E_z. At finite field strength the otherwise degenerate bands are split due to the difference in potential at the two layers. For small fields ($E_z < 0.1\,\mathrm{eV/\mathring{A}}$) the splitting depends linearly on E_z with a slope of around $\pm 0.5\,\mathring{A}$. For larger fields the valence bands deviate from the linear dependence due

---

[1]The MoS_2 monolayer is build up by a hexagonal sheet with the sulfur atoms slightly sticking out of the molybdenum plane. The lattice constant is given by $a_{LDA} = 3.160\,\mathring{A}$ in good agreement to experiment.[31] The bilayer is predominantly bound by van der Waals interaction, the distance of the layers is found to be $d_0 = 2.975\,\mathring{A}$ in experiment[31] (and applied in our calculations), i.e. the distance of centers is $6.147\,\mathring{A}$.
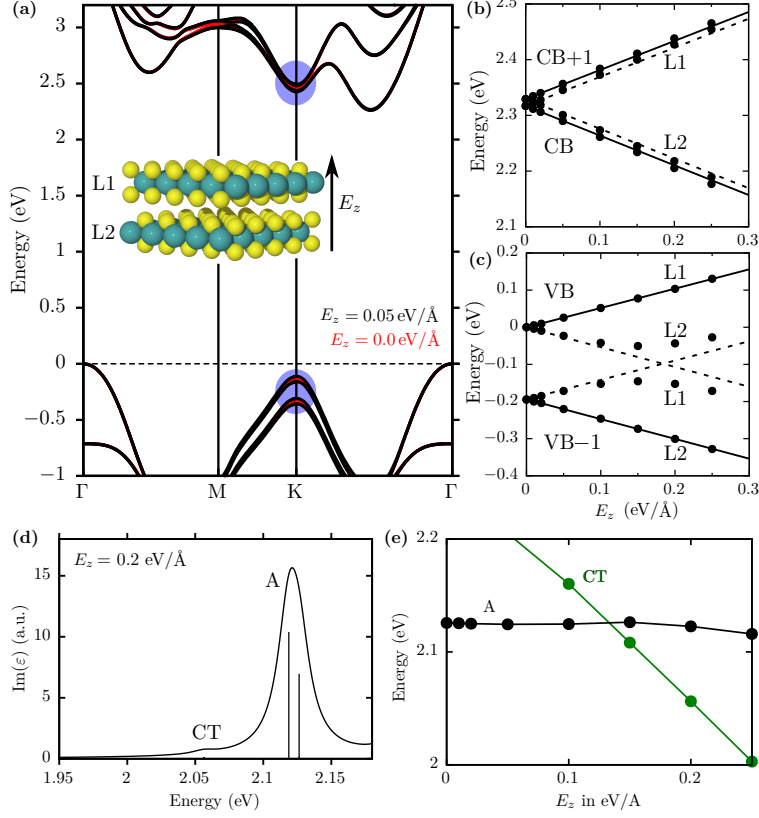
Figure 2: (a) GdW(LDA) band structure for $E_z = 0.0$ (red, mostly covered) and $E_z = 0.05\,\mathrm{eV/Å}$ (black). The bands marked in the blue circles are further investigated in (b) and (c). (b,c) Dependency of the band positions for different fields E_z. The lines are fitted for the uppermost and lowermost points in (c). (d) Absorption spectrum for for $E_z = 0.20\,\mathrm{eV/Å}$. We note that the optical amplitude of the CT state is lower by more than a factor of 100. The exciton peaks (vertical lines) are artificially broadened by $0.01\,\mathrm{eV}$ using Lorentzian functions. (e) Excitation energy of the intralayer A exciton (black) and IL exciton (corresponding to the VB $\rightarrow$ CB transitions on different layers, green).

to an avoided crossing of the spin-split valence bands. Our calculated slope of $1\,\text{Å}$ for the band gap is in good agreement of previous studies of Chu et al.[34] reporting a value of about $1.3\,\text{Å}$ (using $\epsilon_{\mathrm{MoS}_2} \approx 2\epsilon_0$).

The low energy optical spectrum is shown in Fig. 2(d) for an applied field $E_z = 0.2\,\mathrm{eV/Å}$. We find a distinct A exciton peak (of intralayer character) build up by transitions from VB(L1) to CB(L1) and similar transitions in layer 2. At even lower energy we observe a tiny peak resulting from an CT exciton build up by transitions between the VB(L1) and CB(L2). For smaller electric fields (less than $0.15\,\mathrm{eV/Å}$) the interlayer state is found above

6

the intralayer A exciton (see Fig. 2(e)). The IL exciton exciton decreases nearly linearly in E_z ($E^{\mathrm{IL}}(0) - c \cdot E_z$) with a slope of about $1\,\mathrm{eV}/(\mathrm{eV}/\text{Å})$, i.e. the same as the sum of the gradients of the contributing bands. Although the A and IL excitons result form bands at the same position in the Brillouin zone, $E^{\mathrm{IL}}(0) > E^{\mathrm{A}}(0)$; for the MoS_2 bilayer we find a difference of about $0.13\,\mathrm{eV}$. This can be explained by the larger spatial separation of the electron and hole in the IL exciton, which leads to a reduced binding energy.[30] The larger spatial separation (CT type) is also the reason for the much smaller optical signature of the IL exciton (we find that the optical amplitude is lower by more that a factor of 100 in Fig. 2(d)).

We note in passing, that the optical amplitude of CT states reduces drastically with increasing distance (the overlap and thereby the dipole matrix elements decreases exponentially). If the IL distance is increased by more than one Angstrom (or alternatively if a single layer of h-BN is inserted between the MoS_2 layers) our ab-initio calculation leads to dark IL excitations. This is in contrast to experiments of Calman et al.[23] in which bright IL states have been reported for bilayer MoS_2 with three h-BN spacer layers.

To explore the difference of excitons in monolayer and bilayer MoS_2 we follow the evolution of the optical spectrum of the bilayer as the distance between the two layers. In Fig. 3(a) the well known optical absorption spectrum of MoS_2 is shown (bilayer with infinite distance $d = \infty$). We clearly observe the so-called A and B excitons which results form the spin-orbit split valence bands.[33] Furthermore, we observe the excited A_{2s} and the broad above-band gap C exciton as well as dark (triplet) excitons A_d and B_d slightly below the bright counterparts.[6] In the following we will not consider the C and the triplet excitons further but focus on the singlet excitations below the band gap.

For large but finite distances between the two layers [Fig. 3(b)] CT excitons occur in which the electron and hole reside on different layers, see Fig. 4(d). With decreasing distance of the layers all peaks reveal a small red-shift[7] due to the increased screening. However, more interesting, at distances less than four Angstrom (i.e. less than $1\,\text{Å}$ in addition to the
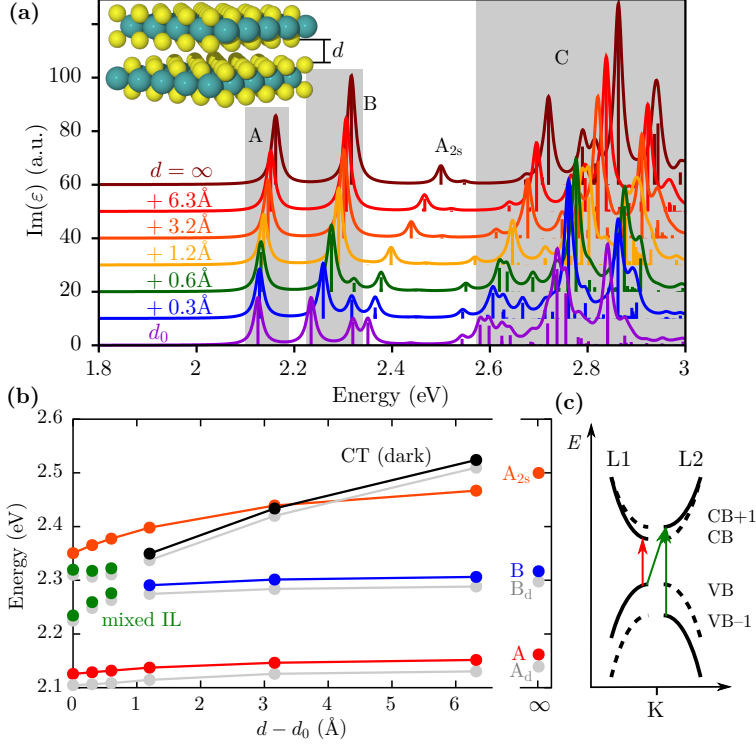
Figure 3: (a) Spectrum of MoS_2 in the transition form monolayer $(d = \infty)$ to bilayer $(d = d_0)$ for various distances. The insert reveals the definition of d as distance between the sulfur atoms. (b) Exciton energy depending on the bilayer distance $d - d_0$. The colors indicate the optically active A, B, and A_{2s} exciton (see (a)) as well as an optically dark charge transfer state (CT). (c) Sketch of the band structure around K. The twice degenerated bands are show left and right for layer 1 (L1) and 2 (L2). The red and green arrows indicate the strongest contributions for the A and mixed IL excitons. The full/dashed bands denote the different spin directions.

optimal distance) a new peak appears at about $2.3\,\mathrm{eV}$ in the spectrum. As we will show in the following this new peak arise due to hybridization of the dark CT exciton with the B intralayer exciton leading to the occurrence of two IL excitons with mixed character (Fig. 1a, right) [2].

All excitons below the band gap result from transitions close to the K point as sketched in Fig. 3(c). Bright excitations have to conserve the spin (the spin direction is indicated by full/dashed bands). For all distances, each band is approximately double degenerate and the corresponding wave functions are localized on mainly one of the two layers L1 or L2.

---

[2]We note that the strong red-shift of the first mixed IL peak results in a reduction of the splitting of the A and B peak from 155 to $110\,\mathrm{meV}$ from monolayer to bilayer while the valence band splitting increases (in GdW) from 175 to $195\,\mathrm{meV}$.
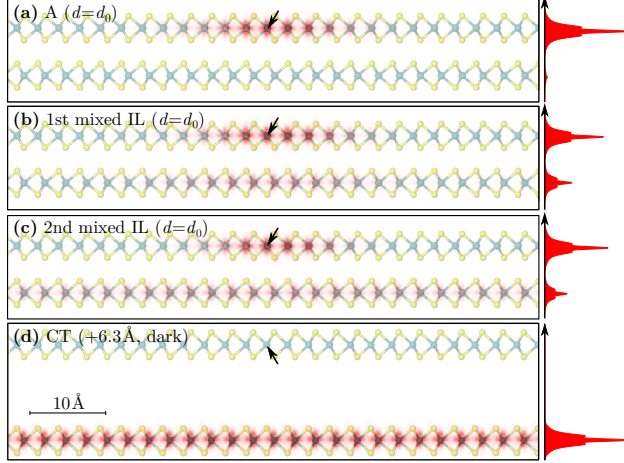
Figure 4: Exciton wave function of the optical active (a) A exciton, (b-c) mixed IL excitons, and (d) the dark CT state (at $d - d_0 = 6.3\,\text{Å}$). The hole is fixed in the upper layer and the electron probability is integrated. The inserts show the result averaged in second direction of the sheets. Note that the results are inverted if the hole is fixed in the lower layer.

The vertical arrows denote the main contributions from the intralayer A and the mixed IL exciton. While the A exciton results from transitions between VB and CB in the same layer, the mixed IL states also involve transitions to the other layer as well (green arrows in Fig. 3(c)). Note that a detailed analysis reveals a tiny splitting of the bonding and anti-bonding states of the two layers (i.e. positive and negative linear combinations) due to the small but non-vanishing interlayer coupling [3].

To scrutinize the character of the mixed IL excitons (2nd and 3rd peaks in the optical spectrum) we calculate the exciton wave function in real space. The exciton wave function can be written as

$$\Phi^S(x_h, x_e) = \sum_{\mathbf{vc}} B^S_{\mathbf{vc}} \phi^*_{\mathbf{v}}(x_h)\phi_{\mathbf{c}}(x_e),$$

where S denotes the exciton and $B^S_{\mathbf{vc}}$ are its coefficients obtained by the diagonalization of the Bethe-Salpeter equation.[35,36] The indices $\mathbf{v}$ and $\mathbf{c}$ denote the combined indices for the band and the momentum. In Fig. 4 we have fixed the hole in the upper layer and evaluated

---

[3]See the Supplementary Material for the discussion of coupling, the model for the hybridisation, and further numerical results at http://www.xxx.org/.

corresponding electron probability. For the intralayer A exciton the electron resides in the same layer as the fixed hole (Fig. 4(a)), i.e. it remains the same character which is observed in the monolayer. In contrast to this, the mixed IL excitons show a distinct amplitude on both layers (Fig. 4(b,c)). The bare CT state, on the other hand, is shown in Fig. 4(d) for a distance of $6.3\,\text{Å}$ and reveals a complete separation of electron and hole. At $d = d_0$ the contribution from the VB-1 to the mixed IL states largely decreased and the main contribution stems from VB(L1)$\rightarrow$CB$+1$(L2). We stress that all exciton states are symmetric under (L1$\leftrightarrow$L2), i.e. fixing the hole in the lower layer inverts the electron distribution in Fig. 4. A more detailed discussion of the CT/intralayer character at different distances can be found in the supplement. We note in passing that the optically dark states (grey in Fig. 3(b)) show a similar mixing.

To get further insight we have set up a simple model to describe the mixing of intralayer and interlayer CT exciton in this study. In Fig. 1(b) a sketch of the initial situation is shown. Two intralayer excitons A and B and their corresponding CT excitations are present. While the CT excitations change with the IL distance, intralayer states are nearly constant. If the intralayer and the CT are close in energy they eventually form mixed IL states. In the following we concentrate on the mixing of B and CT(A), however we note that applying a sufficient large field can be used to couple the CT states to other intralayer states. We describe the excitons in terms of basis states consisting of the uncoupled intralayer and CT excitons. The intralayer exciton on layer i is described by its wave function $|\Psi_{ii}\rangle$, while CT states between the layers i and j are given by $|\Psi_{ij}\rangle$. For an N-layer van der Waals material this leads to N intralayer and $N(N-1)$ interlayer basis states. For a more detailed discussion see the supplemental material. The physical origin of the coupling are the direct IL wave function overlap and the electron-hole exchange interaction between different layers. However, the exchange coupling is small (at least for small momentum transfers[4]) in TMDCs and neglected in the following.

For the current example of bilayer MoS$_2$ ($N = 2$) and focusing on intralayer (B) and CT
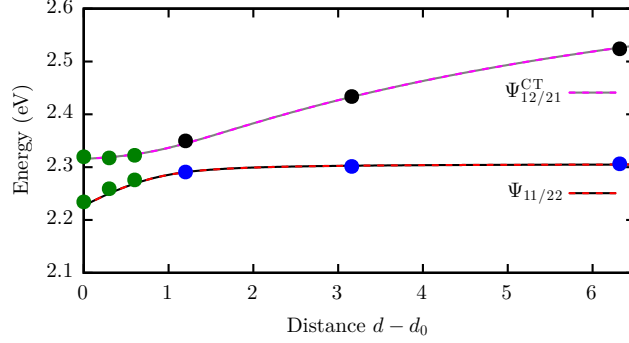
Figure 5: Result of the model for mixed IL states (hybridisation of the B exciton and the CT state). The labels refer to the character of the states for $d \gg d_0$. The points are the ab-initio results replotted from Fig. 3. For further details results see the supplemental material.

(A) excitons, we obtain a 4×4 matrix

$$
H = \begin{pmatrix} E_{11} & 0 & 0 & \vartheta_h \\ 0 & E_{22} & \vartheta_h & 0 \\ 0 & \vartheta_h & E_{12} & 0 \\ \vartheta_h & 0 & 0 & E_{21} \end{pmatrix} \begin{matrix} (\leftrightarrow \Psi_{11}) \\ (\leftrightarrow \Psi_{22}) \\ (\leftrightarrow \Psi_{12}) \\ (\leftrightarrow \Psi_{21}) \end{matrix} \left. \begin{matrix} \\ \\ \\ \\ \end{matrix} \right\} \begin{matrix} \text{intralayer} \\ \\ \text{CT} \end{matrix}
\tag{1}
$$

Here, the exciton energies are given by $E_{11} = E_{22} = E^{\mathrm{B}}$ (intralayer B excitons) and $E_{12} = E_{21} = E^{\mathrm{CT}} + \frac{C}{d}$ (CT states) depending on the distance d. ϑ_h denotes the non-vanishing tunneling for holes, while the tunneling for electrons or both particles simultaneously can be neglected. In total this amounts to four parameters which are extracted (energies) or fitted (tunneling) to our ab-initio calculations. By diagonalizing H we find the four exciton eigenstates and corresponding energies shown in Fig. 5. For large distances we can classify them as the original B and CT excitons. At distances of about $4\,\text{Å}$ the energies of the intralayer and CT states align and new hybridised states with mixed character form and reproduces our ab-initio results very well. In particular it explains the presence of two optically active peaks (or a split peak) which large contributions from the same transitions.

We note that in our model the hybridisation is not limited to the bilayer. On the contrary, we expect mixed IL states in homogeneous and heterogeneous multilayer and bulk to form
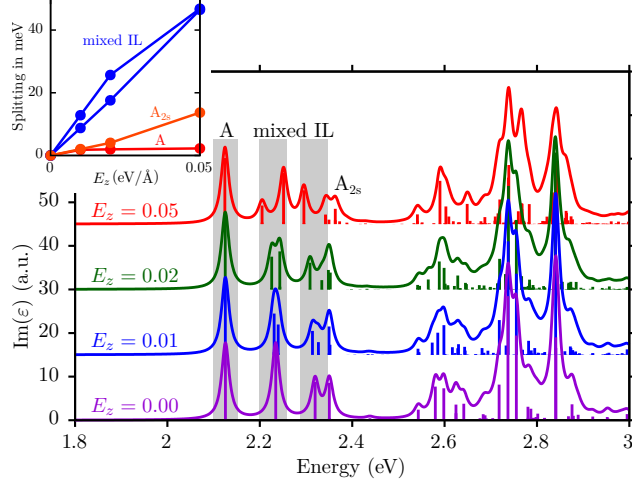
11

Figure 6: Absorption spectrum for different fields E_z (in eV/Å) for $d = d_0$. The spectra are vertically shifted for clarity. The insert shows the shift of the A, mixed IL, and A_{2s} peak.

if intralayer and CT states are close in energy. In particular the model Hamiltonian (1) is also valid for the bulk (2H phase) with two layers in the unit cell (see Supplement of Ref.[25] for bulk MoS_2). Similar models have been previously used to describe bilayer TMDCs[26,29] as well as few-layer systems.[27,28]

To illustrate the different physical nature of the intralayer A and mixed IL excitons we explore their response to a perpendicular electric field. This field breaks the inversion symmetry of the system and the previously doubly degenerate states split up. We note that such a field may be naturally present in experiments on TMDCs due to substrate interactions.[37]

The resulting optical absorption spectra in the presence of different electric fields are shown in Fig. 6. For comparison the spectrum for vanishing field is shown with its four low lying A, mixed IL, and A_{2s} peaks (compare Fig. 3). If E_z is applied the A exciton remains almost unchanged. In contrast, a distinct splitting of the mixed IL peaks (and A_{2s}) is observed. At a field strength of $E_z = 0.05\,\mathrm{eV/Å}$ the mixed IL peaks split by $46\,\mathrm{meV}$. The splitting is nearly linear in E_z (see insert) and has a gradient of about 1 meV/(meV/Å).

These observations can be largely understood from the spatial form of the excitons. As the A exciton is mostly located in one layer, a rigid shift of both VB and CB in one layer

12

(L1 or L2) has only a marginal influence. On the other hand, the mixed IL excitons constitute significant interlayer character (from CT states). As layers 1 and 2 are involved their single-particle band-structure contributions decrease/increase by about $50\,\mathrm{meV}$ (Fig. 2(b,c)). Consequently, the mixed IL states shift by $\pm 23\,\mathrm{meV}$ (splitting $46\,\mathrm{meV}$). We note in passing that the A_{2s} exciton only reveals a splitting at larger fields when their energy is close to those of the mixed IL states. Besides the spectral shift, the corresponding excitonic wave function is modified in an electrical field, i.e. the probability for an electron to reside in the same layer will be different depending on the strength and sign of the electrical field. This behaviour can be also captured in a slightly extended version of the model (1) (see Fig. S3 in the supplement). While A remains unchanged under the application of the field, the electron of the energetically lower mixed IL peak resides in layer L2.

Due to the character of the mixed IL excitons their spatial shape can be tuned in a perpendicular electrical field. By changing the sign of the field the localization of electrons and holes may be easily reversed (i.e. if they reside on the upper or lower layer), while much larger fields are required for CT excitons in heterostructures like MoS_2-$MoSe_2$.[20,30,38]

In summary, we have discussed two different types of IL excitons – the CT type with electron and hole separated and the novel mixed IL type in which CT and intralayer excitons are hybridised. In contrast to the optically dark CT states, the mixed IL excitons have significant optical strength determined by their relative weight of intralayer and CT excitons. In the bilayer MoS_2 we observe mixed IL states which can be tuned into CT excitons by applying a perpendicular electric field. We demonstrated that the formation of mixed IL excitons in multilayer van der Waals structures can be described by a simple tight binding-like exciton model. The concept of mixed IL excitons is important, not only for rationalizing the optical properties of known van der Waals structures, but also for guiding the design of novel heterostructures with strong or tailored optical response.

Supporting Information

Computational details, decomposition of excitons in intralayer and charge transfer character,

further details on the model (Eq. (1)) for the exciton hybridisation, exciton wave function in an electric field. (PDF)

Acknowledgements

Notes

The authors declare no competing financial interest.

References

(1) Castellanos-Gomez, A. Why All the Fuss about 2D Semiconductors? *Nat. Photonics* **2016**, *10*, 202–204.

(2) Komsa, H.-P.; Krasheninnikov, A. V. Effects of Confinement and Environment on the Electronic Structure and Exciton Binding Energy of MoS 2 from First Principles. *Phys. Rev. B: Condens. Matter Mater. Phys.* **2012**, *86*.

(3) Andersen, K.; Latini, S.; Thygesen, K. S. Dielectric Genome of van Der Waals Heterostructures. *Nano Lett.* **2015**, *15*, 4616–4621.

(4) Thygesen, K. S. Calculating Excitons, Plasmons, and Quasiparticles in 2D Materials and van Der Waals Heterostructures. *2D Materials* **2017**, *4*, 022004.

(5) Raja, A.; Chaves, A.; Yu, J.; Arefe, G.; Hill, H. M.; Rigosi, A. F.; Berkelbach, T. C.; Nagler, P.; Schüller, C.; Korn, T.; Nuckolls, C.; Hone, J.; Brus, L. E.; Heinz, T. F.; Reichman, D. R.; Chernikov, A. Coulomb Engineering of the Bandgap and Excitons in Two-Dimensional Materials. *Nature Communications* **2017**, *8*, 15251.

(6) Deilmann, T.; Thygesen, K. S. Dark Excitations in Monolayer Transition Metal Dichalcogenides. *Phys. Rev. B: Condens. Matter Mater. Phys.* **2017**, *96*, 201113.

(7) Drüppel, M.; Deilmann, T.; Krüger, P.; Rohlfing, M. Diversity of trion states and substrate effects in the optical properties of an MoS$_2$ monolayer. *Nat. Commun.* **2017**, *8*, 2117.

(8) Homan, S. B.; Sangwan, V. K.; Balla, I.; Bergeron, H.; Weiss, E. A.; Hersam, M. C. Ultrafast Exciton Dissociation and Long-Lived Charge Separation in a Photovoltaic Pentacene–MoS2 van der Waals Heterojunction. *Nano Letters* **2016**, *17*, 164–169.

(9) Low, T.; Chaves, A.; Caldwell, J. D.; Kumar, A.; Fang, N. X.; Avouris, P.; Heinz, T. F.; Guinea, F.; Martin-Moreno, L.; Koppens, F. Polaritons in Layered Two-Dimensional Materials. *Nat. Mater.* **2016**, *16*, 182–194.

(10) Danovich, M.; Zólyomi, V.; Fal'ko, V. I. Dark Trions and Biexcitons in WS2 and WSe2 Made Bright by E-e Scattering. *Scientific Reports* **2017**, *7*, 45998.

(11) Wang, C.-Y.; Guo, G.-Y. Nonlinear Optical Properties of Transition-Metal Dichalcogenide MX2 (M = Mo, W; X = S, Se) Monolayers and Trilayers from First-Principles Calculations. *The Journal of Physical Chemistry C* **2015**, *119*, 13268–13276.

(12) Onga, M.; Zhang, Y.; Ideue, T.; Iwasa, Y. Exciton Hall effect in monolayer MoS2. *Nat. Mater.* **2017**, *16*, 1193–1197.

(13) Molina-Sánchez, A.; Hummer, K.; Wirtz, L. Vibrational and Optical Properties of MoS2: From Monolayer to Bulk. *Surface Science Reports* **2015**, *70*, 554–586.

(14) Fu, Q.; Nabok, D.; Draxl, C. Energy-Level Alignment at the Interface of Graphene Fluoride and Boron Nitride Monolayers: An Investigation by Many-Body Perturbation Theory. *The Journal of Physical Chemistry C* **2016**, *120*, 11671–11678.

(15) Latini, S.; Olsen, T.; Thygesen, K. S. Excitons in van Der Waals Heterostructures: The Important Role of Dielectric Screening. *Physical Review B* **2015**, *92*, 245123.

(16) Schmitt-Rink, S.; Miller, D. A. B.; Chemla, D. S. Theory of the linear and nonlinear optical properties of semiconductor microcrystallites. *Physical Review B* **1987**, *35*, 8113–8125.

(17) Eisenstein, J. P.; MacDonald, A. H. Bose–Einstein Condensation of Excitons in Bilayer Electron Systems. *Nature* **2004**, *432*, 691–694.

(18) Min, H.; Bistritzer, R.; Su, J.-J.; MacDonald, A. H. Room-Temperature Superfluidity in Graphene Bilayers. *Phys. Rev. B: Condens. Matter Mater. Phys.* **2008**, *78*, 121401.

(19) Li, Y.-M.; Li, J.; Shi, L.-K.; Zhang, D.; Yang, W.; Chang, K. Light-Induced Exciton Spin Hall Effect in van Der Waals Heterostructures. *Phys. Rev. Lett.* **2015**, *115*, 166804.

(20) Ceballos, F.; Bellus, M. Z.; Chiu, H.-Y.; Zhao, H. Ultrafast Charge Separation and Indirect Exciton Formation in a MoS2–MoSe2 van Der Waals Heterostructure. *ACS Nano* **2014**, *8*, 12717–12724.

(21) Gong, Y.; Lin, J.; Wang, X.; Shi, G.; Lei, S.; Lin, Z.; Zou, X.; Ye, G.; Vajtai, R.; Yakobson, B. I.; Terrones, H.; Terrones, M.; Tay, B. K.; Lou, J.; Pantelides, S. T.; Liu, Z.; Zhou, W.; Ajayan, P. M. Vertical and In-Plane Heterostructures from WS2/MoS2 Monolayers. *Nat. Mater.* **2014**, *13*, 1135–1142.

(22) Rivera, P.; Seyler, K. L.; Yu, H.; Schaibley, J. R.; Yan, J.; Mandrus, D. G.; Yao, W.; Xu, X. Valley-Polarized Exciton Dynamics in a 2D Semiconductor Heterostructure. *Science* **2016**, *351*, 688–691.

(23) Calman, E. V.; Fogler, M. M.; Butov, L. V.; Hu, S.; Mishchenko, A.; Geim, A. K. Indirect excitons in van der Waals heterostructures at room temperature. *arXiv* **2017**, 1709.07043v1.

(24) Tanaka, M.; Fukutani, H.; Kuwabara, G. Excitons in VI B Transition Metal Dichalcogenides. *J. Phys. Soc. Jpn.* **1978**, *45*, 1899–1904.

(25) Arora, A.; Drüppel, M.; Schmidt, R.; Deilmann, T.; Schneider, R.; Molas, M. R.; Marauhn, P.; Potemski, M.; Rohlfing, M.; Bratschitsch, R. Interlayer Excitons in a Bulk van Der Waals Semiconductor. *Nat. Commun.* **2017**, *8*, 639.

(26) Gong, Z.; Liu, G.-B.; Yu, H.; Xiao, D.; Cui, X.; Xu, X.; Yao, W. Magnetoelectric Effects and Valley-Controlled Spin Quantum Gates in Transition Metal Dichalcogenide Bilayers. *Nat. Commun.* **2013**, *4*, 2053.

(27) Fan, X.; Singh, D. J.; Zheng, W. Valence Band Splitting on Multilayer MoS_2: Mixing of Spin–Orbit Coupling and Interlayer Coupling. *The Journal of Physical Chemistry Letters* **2016**, 2175–2181.

(28) Molas, M. R.; Nogajewski, K.; Slobodeniuk, A. O.; Binder, J.; Bartos, M.; Potemski, M. Optical Response of Monolayer, Few-Layer and Bulk Tungsten Disulfide. *Nanoscale* **2017**, *9*, 13128–13141.

(29) Gao, S.; Yang, L.; Spataru, C. D. Interlayer Coupling and Gate-Tunable Excitons in Transition Metal Dichalcogenide Heterostructures. *Nano Lett.* **2017**, *17*, 7809–7813.

(30) Latini, S.; Winther, K. T.; Olsen, T.; Thygesen, K. S. Interlayer Excitons and Band Alignment in MoS2/hBN/WSe2 van Der Waals Heterostructures. *Nano Lett.* **2016**, *17*, 6b04275.

(31) Böker, T.; Severin, R.; Müller, A.; Janowitz, C.; Manzke, R.; Voß, D.; Krüger, P.; Mazur, A.; Pollmann, J. Band Structure of MoS2, MoSe2, and α - MoTe2: Angle-Resolved Photoelectron Spectroscopy and *Ab Initio* Calculations. *Phys. Rev. B: Condens. Matter Mater. Phys.* **2001**, *64*, 235305.

(32) Mak, K. F.; Lee, C.; Hone, J.; Shan, J.; Heinz, T. F. Atomically Thin MoS_2: A New Direct-Gap Semiconductor. *Phys. Rev. Lett.* **2010**, *105*, 136805.

(33) Qiu, D. Y.; da Jornada, F. H.; Louie, S. G. Optical Spectrum of MoS_2: Many-Body Effects and Diversity of Exciton States. *Phys. Rev. Lett.* **2013**, *111*, 216805.

(34) Chu, T.; Ilatikhameneh, H.; Klimeck, G.; Rahman, R.; Chen, Z. Electrically Tunable Bandgaps in Bilayer MoS2. *Nano Letters* **2015**, *15*, 8000–8007.

(35) Strinati, G. Dynamical Shift and Broadening of Core Excitons in Semiconductors. *Phys. Rev. Lett.* **1982**, *49*, 1519–1522.

(36) Rohlfing, M.; Louie, S. G. Electron-Hole Excitations and Optical Spectra from First Principles. *Phys. Rev. B: Condens. Matter Mater. Phys.* **2000**, *62*, 4927–4944.

(37) Mak, K. F.; He, K.; Lee, C.; Lee, G. H.; Hone, J.; Heinz, T. F.; Shan, J. Tightly Bound Trions in Monolayer MoS_2. *Nat. Mater.* **2013**, *12*, 207–211.

(38) Zhang, C.; Chuu, C.-P.; Ren, X.; Li, M.-Y.; Li, L.-J.; Jin, C.; Chou, M.-Y.; Shih, C.-K. Interlayer Couplings, Moiré Patterns, and 2D Electronic Superlattices in MoS_2 /WSe_2 Hetero-Bilayers. *Sci. Adv.* **2017**, *3*, e1601459.

Graphical TOC Entry

For TOC only